ABOUT THE EFFICIENCY OF USING "EXTENDED" FOURIER TRANSFORMS FOR SURFACE CHARACTERIZATION BY THE DECONVOLUTION TECHNIQUE

F. Cohen-Tenoudji and G. Quentin
Groups de Physique des Solides, Universite Paris 7,
75221 Paris Cedex 05, France

ABSTRACT

Deconvolution of echoes scattered by a surface tends to give the response function to a Dirac pulse incident on the surface. In some cases, this response function is easily related to the geometry of the scatterer and could be used to characterize it.

In practical, the situation of the Dirac pulse with infinite bandwidth is not realized even by a broad band transducer which acts as a band-pass filter.

We propose here some simple arguments to extend the Fourier spectrum in order to improve the results of deconvolution. Experiments are performed with targets consisting either of small plane surfaces of various shapes or of randomly rough surfaces. Results are in good agreement with those expected using the Kichhoff-Helmholtz integral.

INTRODUCTION

The signal reflected by a surface insonified by a very short ultrasonic pulse contains, in a rather large range of frequencies, information on the scattering properties of the surface. The study of the variation of the scattered signal with frequency can be used to characterize the targets as, for example, defects in metals.[1,2] Indeed, when the dimensions of the target are of the same order of magnitude as the wavelengths of the ultrasonic waves, the scattered signal obeying the diffraction laws is a highly varying function of frequency of which one can infer some dimensions of the scatterer (lengths are estimated within few percent). The targets are generally small and in the far field of the transducers in order that the plane wave approximation can be valid.

The analysis of echoes in the time domain is related to imaging techniques[3] and pulse echo methods are used to get the size of cracks. The methods generally used are high frequency techniques.[4,5] For instance, it was shown by Lloyd[4] who used the Freedman[6] theory on the mechanism of echo formation that one echo signal is generated each time the ultrasonic pulse is incident on a part of the scattering object where a discontinuity appears in the solid angle under which the transducer sees the scattering object. This formulation gives excellent results at high frequencies, when the dimensions of the scattering object are much greater than the ultrasonic wavelength so that the echoes coming from different discontinuities are well separated in the time domain.

Deconvolution of echoes tends to extract information of the whole frequency axis in a given experiment. The method was proposed by Haines and Langston[7] for surface characterization. It tends to recreate the situation where the incident pulse is a Dirac pulse and where the transfer function of the transducers and of the electronic equipment is a constant.

But even broad band transducers delivering band-limiting signals cannot give information on the total frequency axis; it therefore follows that the result of the deconvolution operation can be strongly affected by spurious oscillations. We proposed here to complement the frequency range by extrapolation of the Fourier amplitude toward zero frequency and, moreover, to extend it toward high frequencies by connection of the Fourier complex amplitude of the signal given by a first transducer to that given by a second transducer; the latter working in a higher but connected frequency range than the former.

The technique proposed here is applied to plane targets and to rough surfaces immersed in water.

THEORY

Plane Targets

We first assume that the incident wave can be approximated by a plane wave (experimentally we use a small target placed in the far field of the transducer).

Using the formulation of Neubauer[8] and Johnson[9] of Kirchhoff approximation, the pressure backscattered by a rigid surface A is:

$$p_r(k) = \frac{kBi\alpha}{2\pi} \iint_A R(\theta) \cos\theta \exp(-2ikz)\, da \qquad (1)$$

where α is a phase factor depending on the choice of coordinates, B is a coefficient including the variation of the amplitude spectrum of the incident wave with frequency; da is an elementary area of the scattering surface with z the position of the element da along the axis of propagation of ultrasound Oz; θ is the angle of incidence on the element da; $R(\theta)$ is the reflection coefficient for the angle θ. For a smooth plane target and angle θ is constant and the expression becomes:

$$p_r(k) = \frac{R(\theta) i\alpha k B \cos\theta}{2\pi} \iint_A \exp(-2ikz)\, da \quad . \qquad (2)$$

We can normalize to the value $p_{rq}(k)$ obtained at normal incidence for a calibrated surface A_{cal} placed at the position z_o

$$p_{ro}(k) = \frac{R(0)\, i\alpha k B}{2\pi} A_{cal} \exp(-2ikz_o) \qquad (3)$$

it comes:

$$p_r(k)/p_{ro}(k) = \frac{\beta R(\theta) \cos\theta}{A_{cal} R(0)} \iint_A \exp(-2ikz)\, da \quad . \qquad (4)$$

$\beta = \exp(2ikz_o)$ is a pure phase factor depending on the choice of the origin of coordinates.

For a plane surface A tilted by an angle θ with respect to the ultrasonic beam axis, we choose the axis of coordinates Ox' and Oy in the plane of the surface (Fig. 1).

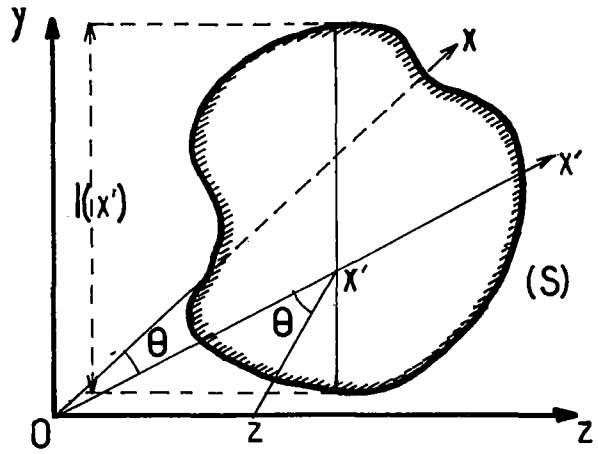

Fig. 1 Scattering geometry.

$x' = z/\sin\theta \qquad da = dx'dy = dy\, dz/\sin\theta$

The integration for the variable y is straightforward and leads to

$$F(k) = \frac{P_r(k)}{P_{ro}(k)} = \frac{\beta R(\theta)}{A_{cal} R(0) \operatorname{tg}\theta} \int_{z_1}^{z_2} l(x') \exp(-2ikz)\, dz. \qquad (5)$$

$l(x')$ is the length of the surface at abscissa x' located at position $z = x' \sin\theta$ along the direction of propagation.

Instead of using the space variables, one can use time and frequency[7] by writing $t = 2z/c$; t is the time taken by the wave to make twice the distance between the origin of coordinates and the height z. So that F(k) becomes:

$$F(f) = \frac{c\, R(\theta)\, \beta}{2A_{cal} R(0) \operatorname{tg}\theta} \int_{t_1}^{t_2} l\left(\frac{ct}{2}\right) \exp(-2i\pi ft)\, dt. \qquad (6)$$

The complex value of F(f) appears to be proportional to the Fourier transform of the length $l(ct/2)$ of the strip of the surface insonified by the wave at time t/2. It is, in principle, possible to evaluate the shape of the scatterer by obtaining $l(ct/2)$ making an inverse Fourier transform of (f):

$$l\left(\frac{ct}{2}\right) = \frac{2R(0) A_{cal} \operatorname{tg}\theta}{c\, R(0)\, \beta} \int_{-\infty}^{+\infty} F(f) \exp(2i\pi ft)\, df. \qquad (7)$$

This inversion supposes that F(f) is known on the total frequency axis; real ultrasonic equipments are band limited so that if one uses instead of F(f) a restriction $F_1(f)$ of F(f) to a band (f_1, f_2), it may appear on the result of the deconvolution spurious oscillations which distort the signal, the period of these oscillations depending on the boundaries f_1 and f_2 (Appendix A). For example, we have simulated on a computer, the effect of the band limitation when the initial signal is a square (duration 830 nanoseconds).

The Fourier transform of this signal is well known to be of the form $(\sin x)/x$. We shall assume the bandwidth of the equipment used to that of a square bandpass filter which cuts off the $(\sin x)/x$ function. Figure 2a shows the result of the inverse Fourier transform for a bandwidth extending from $f_1 = 0.55$ MHz to $f_2 = 3.08$ MHz. The ratio $f_2/f_1 = 5.6$ is approximately that of a commercially available PZT transducer used in the far field region. Two main features can be seen on this graph:

1. The signal has a zero mean value.
2. Spurious oscillations occur.

The zero mean value is a direct consequence that in the frequency domain the value of $F_1(f)$ is zero at zero frequency. The oscillation has a period corresponding to the cutoff frequency f_1 of the filter. We can improve the result by simulating the use of the reunion of the bandwidths of two transducers 0.7 - 3 MHz, 3 - 16.5 MHz. The two edges of the square are more clearly seen owing to the presence of high frequencies in the band, but there is still the slow oscillation due to the low frequncy cutoff (Fig. 2b).

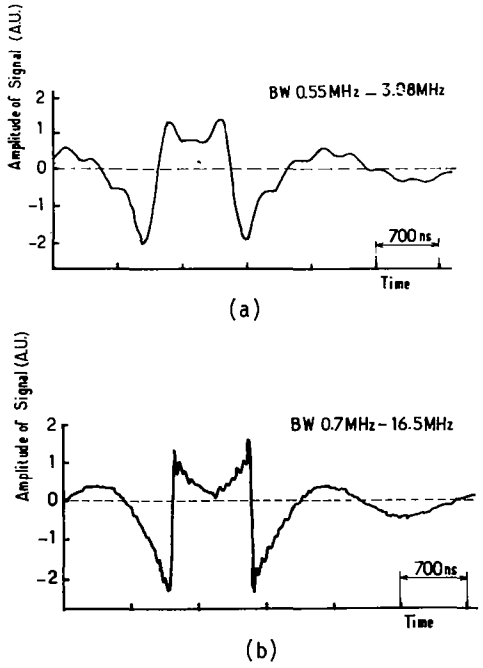

Fig. 2 Computer simulation of the result of band limitation on a reconstruction of a square signal.
a. Bandwidth 0.55 - 3.08 MHz.
b. Bandwidth 0.7 - 16.5 MHz.

Under certain approximations, it is possible to calculate the behavior of the frequency spectrum in the low frequency region. Formula (6) can be written:

$$F(f) = \frac{c\,R(\theta)}{2A_{cal}R(0)tg\theta}\int_{t_1}^{t_2} 1(ct/2)\exp[-2i\pi f(t-t_o)]dt, \quad (8)$$

$t_1/2$ and $t_2/2$ are the times where the wavefront reaches the two extreme edges of the target. The first minimum of the function $|F(f)|$ is generally obtained for a frequency of the order of $f_0 = 1/(t_2-t_1)$. If the lower limit of the band f_1 is less than f_0, for example $f_1 = f_0/2$, the function $F(f)$ will be monotonic for $f < f_1$, and we can use a polynomial expansion of $F(f)$.

Indeed, if we expand in a series the exponential in (8) and if we limit the expansion to the first three terms, when $2\pi f(t-t_o) \ll 1$, it comes:

$$F(f) \simeq D\int_{t_1}^{t_2} 1(ct/2)[1-2i\pi f(t-t_o) -2\pi^2f^2(t-t_o)^2]\,dt$$

$$\simeq D[\int_{t_1}^{t_2} 1(ct/2)dt-2i\pi f\int_{t_1}^{t_2} 1(ct/2)(t-t_o)dt -2\pi^2f^2\int_{t_1}^{t_2} 1(ct/2)(t-t_o)^2dt]+ \ldots \quad (9)$$

with

$$D = \frac{c\,R(\theta)}{2A_{cal}R(0)tg\theta} \quad ;$$

t_o, the time position of the reference surface can be chosen; we will take it so that the second integral in the bracket vanishes; Eq. (9) becomes:

$$F(f) \simeq D[\int_{t_1}^{t_2} 1(ct/2)dt-2\pi^2f^2\int_{t_1}^{t_2} 1(ct/2)(t-t_o)^2dt]. \quad (10)$$

It appears on the last equation that the frequency spectrum is real in the low frequency limit and varies paravolically. We can use this result to reconstruct the low frequency content on a real frequency spectrum. In order to do this we connect the lowest frequency point of the experimental spectrum $F(f_1)$ to the value:

$$F(f = 0) = \frac{R(\theta)\cos\theta\, A}{R(0)A_{cal}}$$

which is known if θ and the area A are known; the area A can be determined by evaluating at normal incidence the ratio of the scattered pressure by surface A to that scattered by the calibration surface A_{cal}. We will connect these two known values by a parabola. The validity of the approximatino depends on the lowest frequency experimentally available and on the length of the surface in the direction of the ultrasonic beam; the following inequality should be verified:

$$2\pi f(t-t_o) \simeq \frac{2\pi Lf\sin\theta}{c} = 2\pi\frac{L}{\lambda}\sin\theta \ll 1$$

where L is the maximum length of the surface along Ox'. The condition being less stringent for a surface with an axis of symmetry along Oy for which the first term ignored proportional to f^3 is zero. This extrapolation toward low frequencies has been made on the spectra corresponding to those of Fig. 2. The results are plotted on Fig. 3a and 3b.

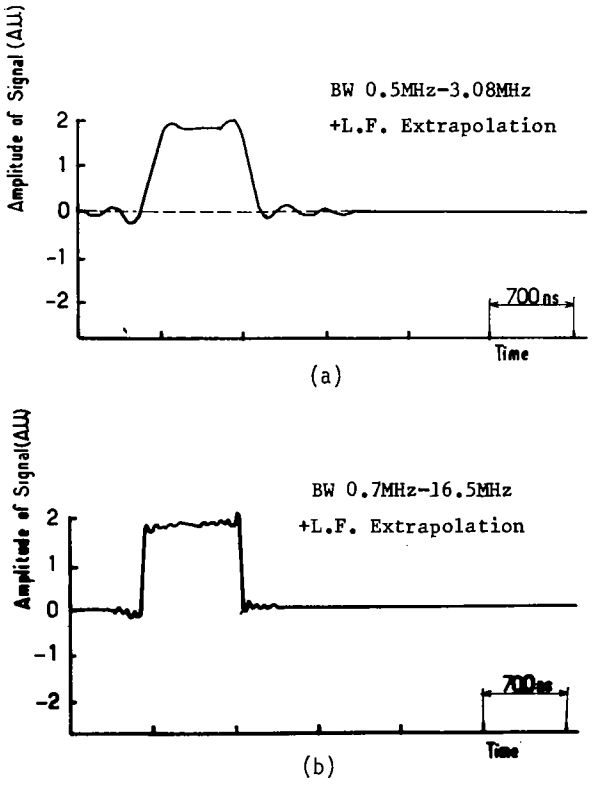

Fig. 3 Improvement of result by low frequency extrapolation.
a. BW 0.5 - 3.08 MHz
b. BW 0.7 - 16.5 MHz

Figure 3a corresponds to the narrower bandwidth of Fig. 2a; the mean value is no longer zero but it is the exact mean value of the signal; the square shape is only distorted by the highest frequency cutoff of the equipment (assumed to be 3 MHz). In Fig. 3b, the square shape of the target is very closely reproduced in the time domain; the only remaining defect is the small spurius oscillation at the highest cutoff frequency (16.5 MHz).

These computer simulations show the usefulness to complement the spectrum for a good restitution of shapes. An important point is to reconstruct a good phase function. Indeed, when one connects the results of two transducers, if the origins of time are not the same in the two experiments, it can appear a phase factor difference between the two Fourier amplitude that could cause, if not corrected, an inadequate final result. Likewise, the phase must be continuous between the low frequency extrapolation and the experimental spectrum. If this last condition is not fulfilled, deformation of the signal may occur (Fig. 4).

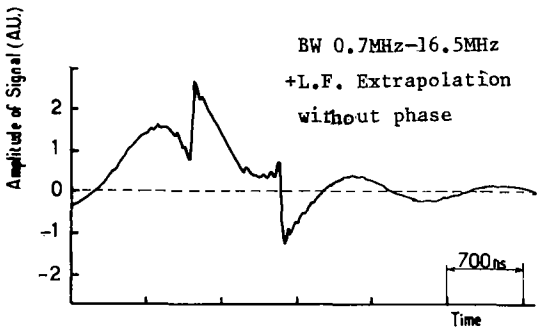

Fig. 4 Effect of a discontinuity in the phase function at the low frequency limit.

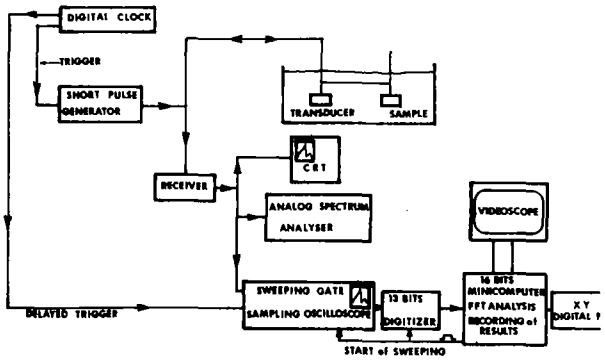

Fig. 5 Experimental equipment.

Rough Surfaces

The method described above can also be applied to the study of randomly rough surfaces. Clay and Medwin[10] have shown that the probability function of heights can be evaluated from backscattered signals at normal incidence. At a given frequency f, the ratio F(f) of the pressure scattered from the rough surface to the pressure reflected by a plane smooth surface is:

$$F(f) = \int_{-\infty}^{+\infty} W(z) \exp(-2ikz)\, dz \quad . \qquad (11)$$

W(z) is the probability density function of heights of the rough surface. By the same transformation as in plane targets, $t = 2z/c$, W(z) appears to be proportional to the inverse Fourier transform of the normalized backscattered signal F(f). So in principle, the application of the deconvolution of extended Fourier domain signals described before leads to an evaluation of the function W(z).

EXPERIMENTAL PROCEDURE

A block diagram of the experimental equipment is given in Fig. 5. The transducer is a highly damped PZT ceramic. It is excited by a very short electrical pulse. The echo backscattered from the surface of the sample is in parallel analyzed by a classical spectrum analyzer and fed to a sampling scope. The output signal is then digitized and sent to a minicomputer PDP 11-03 where the final signal processing is achieved. A 1024 points integer FFT algorithm is used for this process. The backscattered signal is first divided by the reference signal (reflected by a small plane located at the same distance of the transducer). The results obtained with two wide-band transducers exhibiting adjacent bandwidth are connected together and the extrapolation towards lower frequencies is performed. Then the inverse Fourier transform of the frequency domain signal obtained is computed and plotted.

In order to realize approximate plane wave situation, the target is placed in the far field region of the transducer, the diameter of the transducer being greater than that of the target. The targets studied were sections of brass rods, parallelepipedic, cylindrical or other.

The built-up spectrum for a square section is plotted in Fig. 6. The spectrum is made of three parts: the continuous line is the result given by a transducer; the part on the right is given by a second transducer and, the part of the left is obtained by the parabolic extrapolation. In Fig. 7 the continuous line is the result of the deconvolution, the dashed line is the theoretical signal.

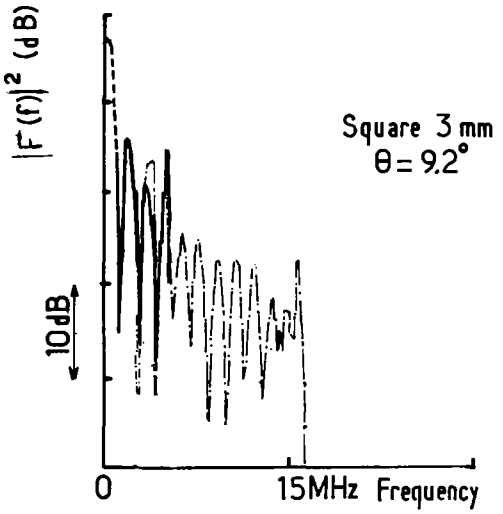

Fig. 6 Reconstructed spectrum for a plane target. —— LF transducer, —·— HF transducer, ---extrapolation.

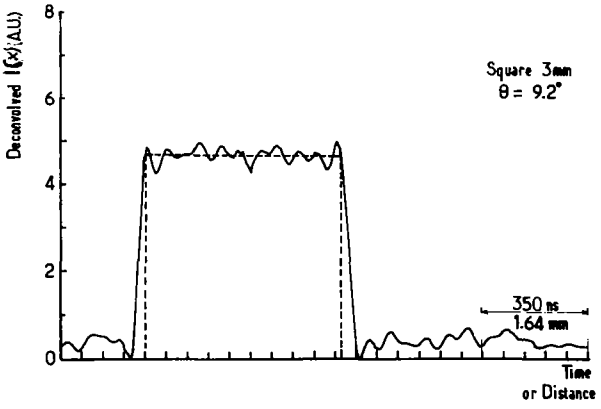

Fig. 7 Deconvolved signal (continuous line) and theoretical signal (dashed line) for a square target.

In Fig. 8, one can see the result of the deconvolution for a rod-section shaped as an M (continuous line); the dashed line is the expected result.

The results obtained for a quasi ellipsoidal section are plotted in Fig. 9. The ratio between the two axis lengths is 2. Figure 9a plots the result when the major axis is horizontal. The amplitude has been adjusted so that the maximum height of the function I(x') is half the width. If one keeps the same vertical scale, and if one conducts the experiment with the major axis vertical, the result of deconvolution should be such that the height is twice the width. This is obtained on the experimental result in Fig. 9b.

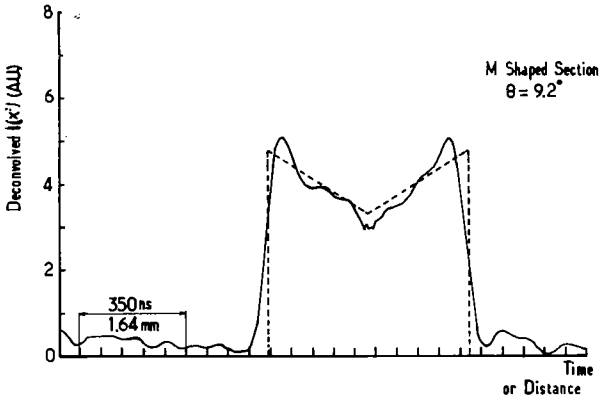

Fig. 8 Deconvolved signal (continuous line) and theoretical signal (dashed line) for an M shaped target.

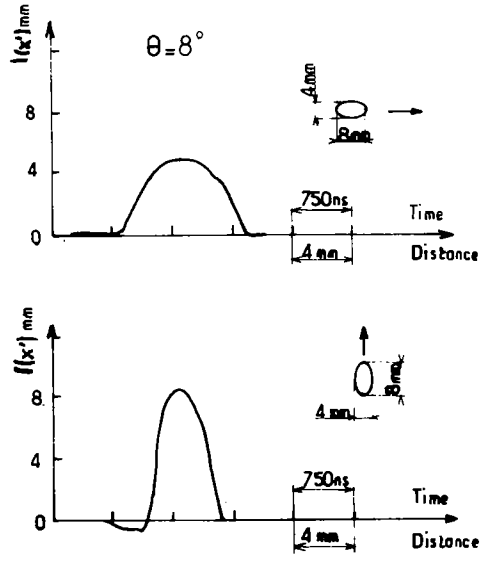

Fig. 9 Deconvolved signal for a quasi-ellipsoidal section. a. Major axis horizontal. b. Major axis vertical.

The results obtained for two samples of the evaluation of the probability density function of the heights are plotted in Figs. 10 and 11. The dotted lines are obtained by mechanical measurements. The continuous lines are the results of the ultrasonic measurements. For that case as for plane targets, the results are satisfactory.

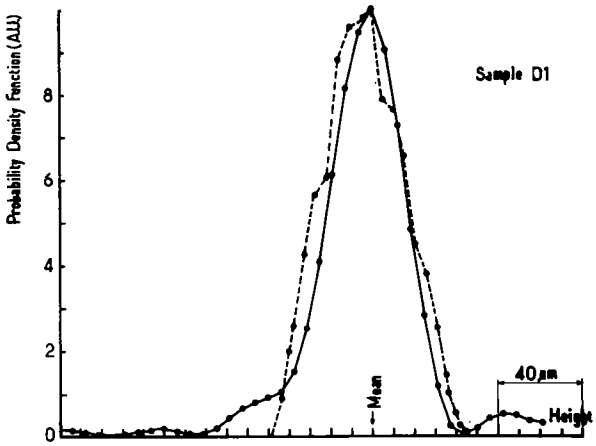

Fig. 10 Probability density function of sample D1. --- Mechanically measured, —— ultrasonic measurement.

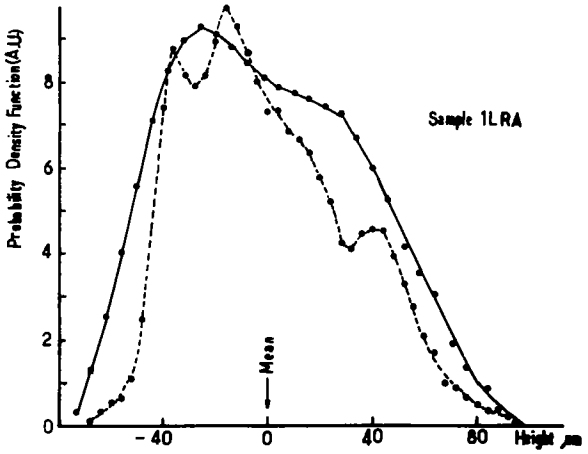

Fig. 11 Probability density function of sample 1LRA. --- Mechanically measured, —— ultrasonic measurement.

CONCLUSION

We have studied the filtering effect operated by a transducer on the ideal response function of a target to an incident Dirac pulse. The extension of the frequency bandwidth leads to satisfactory results. The method could be useful to complete existing ones for characterization of plane surfaces. This method could be useful for the characterization of plane defect in materials. First results in that direction are promising.

APPENDIX A

Let h(t) be a real function of time and F(f) its Fourier transform:

$$F(f) = \int_{-\infty}^{+\infty} h(t) \exp(-2i\pi ft)\, dt \qquad (12)$$

F(f) is such that $F(-f) = F^*(f)$. Let us call $F_1(f)$ the function equal to F(f) between f_1 and f_2 and equal to zero elsewhere. $F_1(f)$ can be written

$$F_1(f) = F(f)[H(f+f_2)-H(f+f_1)+H(f-f_1)-H(f-f_2)] \qquad (13)$$

where

$$H(f) = \begin{cases} 0 \text{ if } f < 0 \\ 1 \text{ if } f > 0 \end{cases} .$$

The inverse Fourier transform of $F_1(f)$ is:

$$h_1(t) = h(t) \oplus \left\{ \frac{\sin 2\pi f_2 t}{\pi t} - \frac{\sin 2\pi f_1 t}{\pi t} \right\} . \qquad (14)$$

That is, if we take the inverse Fourier transform of $F_1(f)$ instead of F(f), the result is the convolution product of h(t) by the functions

$$\frac{\sin 2\pi f_2 t}{\pi t} \text{ and } -\frac{\sin 2\pi f_1 t}{\pi t} .$$

REFERENCES

1. O.R. Gericke, Journal of Metals, 18, (8), pp. 932-937, (1966).
2. J.D. Achenbach, L. Adler and D.K. Lewis, Jour. Acoust. Soc. Am., 66, (4) pp. 1848-1856, (1979).
3. G.S. Kino, Proc. IEEE on Acoustic Imaging, 67, pp. 510-525, (1979).
4. E. Lloyd, Ultrasonics International Conference Proceedings, IPC London, pp. 54-57, (1975).
5. J.K. Cohen, N. Bleistein and R.K. Esley, Proc. of the ARPA-AFML Review, pp. 454-458, Jan. 1979.
6. A. Freedman, Acustica, 12,(1), pp. 10-21, (1962).
7. N.F. Haines and D.B. Langston, J. Acoust. Soc. Am., 67, pp. 1443-1454, (1979).
8. W.G. Neubauer, J. Acoust. Soc. Am., 35, 279, (1963).
9. D.M. Johnson, J. Acoust. Soc. m., 59, 1319, (1976).
10. C.S. Clay and H. Medwin, J. Acoust. Soc. Am., 47, 1412, (1970).

J.D. Achenback, Chairman (Northwestern): Let's take time for one question. Is there a quick question? Otherwise, we'll postpone -

Gordon Kino (Stanford): What was the center of the frequency of the two transducers?

Frederick Cohen-Tenoudji (University of Paris): The low frequency transducer was centered at 2.5 megahertz, the high frequency transducer was centered at 8 megahertz. The total bandwidth was approximately from one megahertz to 15 megahertz.

Gordon Kino: Have you worked out the effect of the transverse direction? You're working out shapes from this, so it must depend somehow on how accurately you get the shape, an effect of definition - it's an imaging system.

Federick Cohen-Tenoudju: Yes, I think that the definition will be given by the relation between highest frequency present in the spectrum. We will have the transverse definition given by $\Delta a \simeq \lambda_m/(2 \sin \theta)$ where θ is the angle of incidence and λ_m is the minimum wavelength. That's what I usually see. It results in a spread out on the edge typical of the highest frequency present.

J.D. Achenback, Chairman: I'm sure we'll have to cut off the discussion and move to the next two talks.